Nuclear Instruments and Methods in Physics Research A 648 (2011) S103–S106

Contents lists available at ScienceDirect

Nuclear Instruments and Methods in Physics Research A

journal homepage: www.elsevier.com/locate/nima

Approaches to juxta-pleural nodule detection in CT images within the MAGIC-5 Collaboration

G. De Nunzio [a,*], A. Massafra [b], R. Cataldo [a], I. De Mitri [b], M. Peccarisi [b], M.E. Fantacci [c], G. Gargano [d], E. Lopez Torres [e]

[a] University of Salento, Materials Science Department & Istituto Nazionale di Fisica Nucleare (INFN), Lecce, Italy
[b] University of Salento, Physics Department & Istituto Nazionale di Fisica Nucleare (INFN), Lecce, Italy
[c] University of Pisa, Physics Department & Istituto Nazionale di Fisica Nucleare (INFN), Pisa, Italy
[d] University of Bari, Physics Department & Istituto Nazionale di Fisica Nucleare (INFN), Bari, Italy
[e] CEADEN, Havana, Cuba

ARTICLE INFO

Available online 17 December 2010

Keywords:
Juxta-pleural lung-nodule detection
Computer-Assisted Detection
Medical image processing

ABSTRACT

This work is a part of the MAGIC-5 (Medical Applications on a Grid Infrastructure Connection) experiment of the Italian INFN (Istituto Nazionale di Fisica Nucleare). A simple CAD (Computer-Assisted Detection) system for juxta-pleural lung nodules in CT images is presented, with the purpose of comparing different 2D concavity-patching techniques and assessing the respective efficiency in locating nodules. After a short introduction on the motivation, and a review of some CAD systems for lung nodules already published by the MAGIC-5 Collaboration, the paper describes the main lines of this particular approach, giving preliminary results and comments. In our procedure, candidate nodules are identified by patching lung border concavities in a hierarchical multiscale framework. Once located, they are fed to an artificial neural network for false positive reduction. The system has a modular structure that easily allows the insertion of arbitrary border-smoothing functions for concavity detection and nodule searching. In this paper the α-hull and morphological closing are compared, proving the higher sensitivity of the former, which also appears computationally less heavy.

1. Introduction

1.1. Lung cancer

Lung cancer is one of the main causes [1,2] of death among both men and women. The 5-year survival rate is strictly related to the stage in which the disease is diagnosed [3]—early detection and subsequent resection can significantly improve the prognosis. The development of "Computer-Assisted Detection" (CAD) techniques to automatically locate nodules can enhance diagnosis accuracy in the usual clinical practice [4]. Computed Tomography (CT) is considered to be the best imaging modality for the detection of lung nodules; see e.g. Refs. [5–7].

1.2. Project description

This work is a part of the development of a composite CAD system for the detection of pulmonary nodules in CT scans, carried out in the framework of the "Medical Applications in a Grid Infrastructure Connection" (MAGIC-5) Collaboration, an experiment of the Italian INFN ("Istituto Nazionale di Fisica Nucleare"). Different kinds of tumor nodules may be found in the lung parenchyma—shape, size, and position vary considerably, so that no unique detection approach exists. Dense nodules may be in contact with the pleura ("juxta-pleural" nodules), because either they grew near or originated from the pleural sheet. Segmentation algorithms often fail in returning correct lung borders with all the juxta-pleural nodules included, due to their high density—in this case, nodules appear in the segmentation masks as small border concavities. In this work we focus on the problem of efficiently locating juxta-pleural nodules, comparing the success of two concavity-patching methods in discriminating them from other structures.

The MAGIC-5 lung CAD system already allows the detection of lung nodules, both internal and juxta-pleural, with various approaches and good accuracy, e.g. Refs. [8–12] In particular, concerning juxta-pleural nodules, in Ref. [10] the directional-gradient concentration method is applied to the pleural surface (identified as a triangulated isosurface) and combined with a morphological-opening based procedure to generate a list of pleural nodule candidates. Each candidate is characterized by 12 geometrical and textural features, which are analyzed by a rule-based filter and a neural classifier.

* Corresponding author. Tel.: +390 8322 97084; fax: +390 8322 97100.
E-mail address: giorgio.denunzio@unisalento.it (G. De Nunzio).

0168-9002/$ - see front matter © 2010 Elsevier B.V. All rights reserved.
doi:10.1016/j.nima.2010.12.082

The latter generates a list of CAD findings. Care is devoted to the reduction of false positives (FPs) by the application of a Self Organizing Map (SOM), which helps in identifying a representative subset of the FP population, for efficient network training. In the approach described in Ref. [11] the lung parenchymal volume is segmented by means of a region growing (RG) algorithm, and pleural nodules are included through an original ACM technique. Then, RG is iteratively applied to the previously segmented volume in order to detect candidate nodules. A double-threshold cut and a supervised feed-forward neural network are applied for FP reduction. The *leave-one-out* cross validation is used to exploit the highest possible number of true positives (TP) during the training phase. Finally, in Ref. [12] ant colonies are able to segment artificially-generated and natural objects of different shape, intensity, and background. The CT analysis makes use of a Channeler Ant Model (CAM) to segment the bronchial and vascular tree and remove it from the CT before searching for nodular structures in the image with a dedicated filter. The moving rules depend on the pheromone content at destination. The ant colony behavior is related to the original image features via their influence on the pheromone release rules.

The interest in developing complementary methods comes from the possibility of integrating the results given by diverse procedures with the purpose of obtaining a "composite" CAD system more accurate than each component.[13] Therefore we decided to plan a further system devoted to juxta-pleural nodules—it is based on the α-hull [14,15], a concavity-patching method far less known than its well-spread counterpart, i.e. morphological closing. This explorative paper is our first attempt at the development of an α-hull CAD tool and, while it succeeds in building a working system, it anyway does not try yet to optimize it in terms of classification accuracy, focusing instead on a comparison with morphological closing, with the purpose of selecting the more performing concavity-patching technique. Moreover, the idea of performing nodule search in a hierarchical framework [15] is pursued.

The nodule-inclusion procedure starts from the segmented pulmonary volume, where dense juxta-pleural nodules remain outside the lung mask, and appear as small concavities of the lung border. Following and generalizing Ref. [15], morphological closing and α-hull were implemented in a hierarchical framework, depending on a suitable parameter (the curvature of the circular SE and the α value)—this approach allows a multiscale analysis, by which a tree of nested concavities can be built.

2. Materials and methods

2.1. Materials

The procedure described in this paper was tested on a database composed of 57 high-resolution, low-dose (140 kV, 20 mA) CT scans with internal and juxta-pleural nodules, or belonging to patients without nodules. Slices are 512×512 pixels, 12-bit gray level matrices; pixel size ranges from 0.53 to 0.74 mm in the *xy* axial plane, while *z* size is 1 mm. The images were annotated by experienced radiologists, giving a list of found nodules with position and size. The database contains 78 diagnosed juxta-pleural nodules, of which 28 are in direct contact with the pleura, and the others connected to it by peduncles.

2.2. Methods

Our comparison procedure follows the classical scheme of a CAD system: (a) segmentation of the volume of interest (i.e. the lungs), (b) juxta-pleural candidate nodule detection, (c) feature choice and calculation, and (d) classification. In this work, we stress on stage (b), where candidate nodules are identified by a concavity-patching method, which can be the alpha hull, morphological closing, ACMs, or some other technique to be tested. The features we calculated in step (c) are not necessarily the best—in this preliminary work we chose some reasonable ones (some borrowed from Ref. [15], and some already used in the lung CAD systems developed by the MAGIC-5 Collaboration, e.g. Ref. [11]), with the only purpose of setting up a procedure to discriminate between concavity-patching techniques.

2.2.1. Segmentation

The segmentation algorithm can be found in Ref. [17]. The result is a pair of binary masks for the two lungs. Dense nodules (and vessels) are not contained in the segmented volume. Therefore, regions containing nodules and vessels now show cavities and concavities. The concavities originated by juxta-pleural nodules (and larger vessels) are dealt with in the next phase by concavity-patching procedures that allow concavity (i.e. candidate nodule) detection.

2.2.2. Detection of juxta-pleural candidate nodules

Using a concavity-patching method, which allows the reconstruction of a smoothed lung border (where concavities are "closed"), and by applying a difference operation between the old and the new border, we can detect concavities where the two borders differ. Moreover, if the procedure relies on a spatial parameter (related to a concavity scale), we obtain a multiscale procedure [15], which also retains information about nesting—this can be useful to better understand the relation between concavities (e.g. a nodule being contained in the hilus concavity). In this paper 2D morphological closing and alpha hull are implemented, and the respective efficiencies compared.

Morphological closing is defined as a dilation operation followed by erosion, both using the same structural element (SE). Here a disk with varying radius r is used. The α-hull [14,15] is a convex hull generalization, able to detect concavities, whose shape depends on a curvature parameter α. A definition of α-hull is as follows: given a set S of points in the plane, and a positive number α, the global α-hull of S is the intersection of the closed complements of all the circles of radius $r=1/\alpha$, such that the intersection of these circles with S is empty. By definition, the α-hull when $\alpha=0$ is the convex hull. The effect of calculating the α-hull of a closed and dense spatial distribution of points (such as the segmentation mask of a lung slice) is the gradual closing of concavities, depending on the value of α.

Following and generalizing Ref. [15], morphological closing and α-hull were tested in a hierarchical framework, respectively depending on the inverse of the radius of the SE (the disk), hereafter also called α, and on the α value—this approach allowed a hierarchical, multiscale analysis of concavities, leading to juxta-pleural nodule detection. The programming environment was Matlab R2008a for Linux, with the Image Processing Toolbox. Morphological closing was implemented by the standard toolbox function, while the C code for the α-hull is available on the Web [16].

As pointed out, concavities are found, slice by slice, by calculating the difference between the borders of the original lung slice B, and the smoothed one B_α: $D=B-B_\alpha$. D is a list of pixels belonging to the original border but not to the smoothed one, therefore it consists of groups of pixels identifying the concavities at the α value of the scale parameter. Concavities are spotted by finding groups of contiguous pixels separated by gaps. Fig. 1 shows the result of the described operation on a lung slice at an arbitrary α value, for the α-hull. By repeating, for a suitable set of α values, the difference operation in and the search for concavities, a hierarchy for each slice is determined.

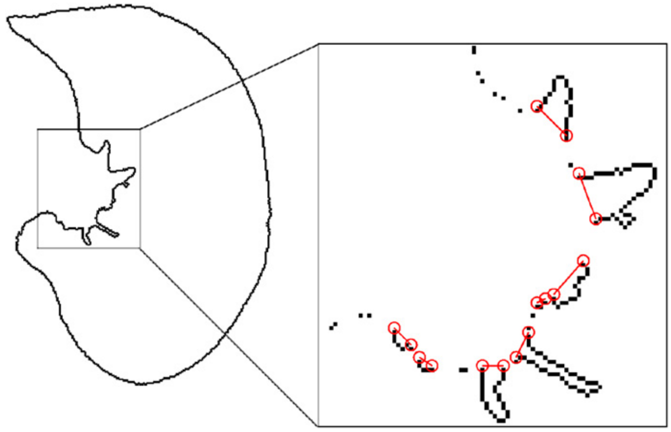

Fig. 1. Concavity detection. A lung slice after concavity detection at an arbitrary α value; concavity-patching technique used for border smoothing (followed by border difference and concavity spotting) was α-hull.

The choice of a useful set A of α values involved much experimenting, because of competing requests—a richer A set means a finer description of concavities, but also longer calculation times and, even, a larger number of *false positives* (FPs). Very small α (large radii) are useless because they reveal noise and are not able to detect nested concavities. Very large α (small radii) are useless too, because they give negligible border difference (no detection). Because of the geometrical meaning of the α parameter (a curvature, i.e. the inverse of a radius) we populated A according to the range of nodule sizes (2–12 mm). In our preliminary tests we arbitrarily used the following five α values: {0.083, 0.100, 0.125, 0.154, 0.182 mm^{-1}}, corresponding to radii equal to about {12, 10, 8, 6.5, 5.5 mm}, because this A set was able to detect most of the nodules. Nevertheless, we realized that small radii would alter feature values—thus we decided to reduce the A set cardinality to three, preserving {0.083, 0.100, 0.125 mm^{-1}}. We verified that this set optimized both nodule-searching sensitivity in the detection phase and classification performance.

2.2.3. Features

After maximizing sensitivity in the detection step, the next goal is the reduction of FPs, i.e. how to identify and reject the concavities that are not juxta-pleural nodules. This task can be obtained by suitable characterizing features calculated on the nodule candidates, which discriminate between nodules and FP. In our simple approach, FP reduction will be performed by straightforward linear filters (thresholds on the feature values), followed by the use of an Artificial Neural Network (ANN). We decided to employ, as a preliminary test, geometrical features (some from Ref. [15]), and first-order gray-value features (like in Ref. [11]). Thus, our set of features was: $F=G\cup T\cup\{\alpha\}$, where α is the scale value at which the concavity was detected and

G={*span*, *depth*, *borderLength*, *area*, *depthOverSpan*, *radius*, *circularity*}
T={*grayMean*, *grayStd*, *graySkew*, *grayKurt*, *grayEntrpy*}

The *span* of a concavity is the length of the segment that joins its extremal points; *depth* is the length of the longest perpendicular segment between the concavity pixels and the segment defining the *span*; *borderLength* is the number of boundary points composing the concavity profile; the *area* is the number of pixels between the *span* segment and the concavity boundary; *depthOverSpan* is *depth*/*span*; the *radius* is the mean distance of the boundary pixels from the concavity centroid; and *circularity* is the ratio of its area A and that of the circle having the same perimeter p (i.e. *borderLength*)—$c=4\pi A/p^2$. First-order textural features are gray mean, standard deviation, skewness, kurtosis, and entropy, calculated for the pixels within the concavity. Feature distributions were examined and gross intervals of values for a preliminary filtering were identified.

2.2.4. Classification

A supervised two-layer, 13-input, 20-hidden-neuron, 1-output feed-forward neural network, trained with gradient descent learning rule with momentum, was chosen as the classifier system. To calculate classification efficiency for each of the concavity-patching methods, we define as *true positives* (TPs) the candidate nodules that meet the radiologists' diagnosis according to the following condition: the Euclidean distance between the centroid of the concavity, and the centroid of a diagnosed nodule, is lower than $1.5r_R$, where r_R is the nodule radius according to the radiologists. All the other candidates are considered to be false positives. The 1.5 factor takes into account the radius measurement uncertainty. K-fold cross validation [18] (with $K=10$) was used. The ANN output, calculated on the concavity list, is distributed in the range [0,1]. By varying a decision threshold, and assigning target $t=1$ to candidates above threshold (probably positive), and $t=0$ to candidates below threshold (probably negative), sensitivity and specificity referred to the known diagnosis can be calculated. By plotting (for each threshold value) sensitivity vs [1-specificity], and smoothly joining points, the Receiver Operating Characteristic (ROC) curve can be drawn.

3. Results

3.1. Execution time of detection step

A CT scan of 300 slices takes about 3 min per α value for the α-hull, quite more (about 10 min) for morphological closing, on a modern Dell Precision T5500 (two quad-core Intel Xeon E5540 at 2.53 GHz, 12 GB RAM).

3.2. Sensitivity of concavity-detection systems

The number of juxta-pleural nodules contained in the set of concavities detected by the α-hull is 72 out of 78, while only 66 are collected by morphological closing (sensitivity—92.3% and 84.6%). All the neglected nodules are not in direct contact with the pleura, but are connected to it by subtle peduncles, with small concavities in the lung border. This fact justifies the failures. All the nodules lost by the α-hull are also lost by the morphological closing. As to the influence of the multiscale approach on detection accuracy, we tried A sets with one element—the result was an increased loss of nodules. On the contrary, increasing A cardinality did not help us recover already lost lesions.

3.3. ROC curves

ROC curve calculation allows quantification of the classifier performance on the collected data, strongly related to the detection method fitness and to the feature choice.

In our tests, the ROC curves for both methods look similar. The area under the curve (AUC), and sensitivity and specificity, in the point where they have the same value, are (0.80, 72%) and (0.84, 75%), respectively. It is remarkable that ROC curves obtained when only one α value is inserted in the A set show AUC values just a little lower (e.g. 0.76), but the curve shape is far less regular. Moreover, using an A set with more than three elements does not give any accuracy enhancement, because the number of FPs increases too.

4. Conclusions and prospects

A CAD system for juxta-pleural nodule detection in thorax CT images was developed, with the purpose of being a test framework for different concavity-patching algorithms used for multiscale nodule localization. Nodule-candidate search is followed by an ANN for FP reduction. In particular, two concavity-patching techniques were compared—the α-hull and morphological closing. At detection level, the former had better sensitivity (92.3% vs 84.6%), marking as positive some nodules connected to the pleura by subtle peduncles, that morphological closing did not see. At the classification level, the two methods proved roughly equivalent, with sensitivity and specificity around 72–75% and AUC around 0.80–0.84. On the other hand, the two approaches really differed in the computational cost—calculation time for morphological closing (at least in the MATLAB implementation) largely exceeds the α-hull. The preceding considerations lead to prefer the latter approach. In conclusion, the α-hull appears to be a powerful method for the detection of concavities.

In the future the system will be applied to a larger number of images, by also diversifying the source (the LIDC database will be used). The Active Contour Model already implemented in the MAGIC-5 framework and described in Ref. [11] will also be tested as an alternative concavity-patching method. Finally, the code will be parallelized to increase efficiency.

Acknowledgments

We wish to acknowledge: F. Falaschi, C. Spinelli, L. Battolla and A. De Liperi of ‘‘U.O. Radiodiagnostica 2’’, Azienda Ospedaliera Universitaria Pisana; D. Caramella, T. Tarantino, and M. Barattini of the ‘‘Divisione di Radiologia Diagnostica e Interventistica’’, Dipartimento di ‘‘Oncologia, Trapianti e Nuove Tecnologie in Medicina’’ dell’Universitá di Pisa, M. Torsello and I. Zecca of the ‘‘U.O. Radiologia’’, Azienda Ospedaliera Vito Fazzi, Lecce, for providing the dataset of CT scans and for useful discussions. This work was carried out in the framework of the MAGIC-5 Collaboration, supported by the Italian ‘‘Istituto Nazionale di Fisica Nucleare’’ (INFN, CSN 5) and by the Italian ‘‘Ministero dell’Istruzione, dell’ Universitá e della Ricerca (MIUR)’’.

References

[1] The Lancet, vol. 365, May 14, 2005.
[2] A.J. Alberg, J.M. Samet, Chest 123 (2003).
[3] G. Picozzi, et al., Radiologia Medica (Torino) 109 (1–2) (2005) 17 See also 〈http://www.cspo.it/〉.
[4] B. Sahiner, et al., Academic Radiology 16 (12) (2009) 1518.
[5] E.R. Heitzman, Chest 4 (1986) 237S89 4 (1986) 237S.
[6] M.A. Howe, B.H. Gross, Computer Radiology 11 (1987) 61.
[7] M. Remy-Jardin, et al., Radiology 187 (1993) 513.
[8] I. Gori, et al., Journal of Instrumentation 2 (2007) P09007.
[9] A. Retico, et al., Computers in Biology and Medicine 38 (4) (2008) 525.
[10] A. Retico, et al., Computers in Biology and Medicine 39 (2009) 1137.
[11] R. Bellotti, et al., Medical Physics 34 (12) (2007) 4901.
[12] P. Cerello, et al., Pattern Recognition (2009). doi:10.1016/j.patcog.2009.10.007.
[13] B. van Ginneken, et al., Medical Image Analysis 14 (6) (2010) 707.
[14] H. Edelsbrunner, et al., IEEE Transactions On Information Theory IT-29 (4) (1983) 551.
[15] W.F. Sensakovic, et al., A general method for the identification and repair of concavities in segmented medical images, in: Proceedings of the Medical Image Conference 2008, Dresden.
[16] 〈www.netlib.org/voronoi/hull.html〉 (see also weblog.bocoup.com/compiling-clarksons-hull-in-os-x).
[17] G. De Nunzio, et al., Journal of Digital Imaging (2009) 10–20. doi:10.1007/s10278-009-9229-11 ISSN0897-1889 (print) 1618-727X (online).
[18] M. Stone, Journal of the Royal Statistical Society. Series B Statistical Methodology 36 (1974) 111.